



NDE2002 predict. assure. improve.  
National Seminar of ISNT  
Chennai, 5. – 7. 12. 2002  
www.nde2002.org

## Experimental verification of model-based interpretation of the bobbin coil ECT signal for quantitative characterization in NPP SG tubes

Sung-Jin Song<sup>1</sup>, Young H. Kim<sup>1</sup>, Eui-Lae Kim<sup>1</sup>, Young Hwan Choi<sup>2</sup>

<sup>1</sup>School of Mechanical Engineering, Sungkyunkwan University Suwon, 440-746 Korea <sup>2</sup>Nuclear Safety Research Dept., Korea Institute of Nuclear Safety, Taejeon, 305-338 Korea

**ABSTRACT.** The model-based inversion tools for eddy current signals have been developed by the novel combination of neural networks and finite element modeling for quantitative flaw characterization in steam generator tubes. In the present work, interpretation of experimental eddy current signals was carried out in order to validate the developed inversion tools. A database was constructed using the synthetic flaw signals generated by the finite element modeling. The hybrid neural networks of a PNN classifier and BPNN size estimators were trained using the synthetic signals. Experimental eddy current signals were obtained from axisymmetric artificial flaws. Interpretations of flaws were carried out by feeding experimental signals into the neural networks. The results of interpretations were excellent, so that the developed inversion tools would be applicable to the interpretation of experimental eddy current signals.

### INTRODUCTION

Steam generator (SG) tubes play a very important role in the operation of nuclear power plants (NPP) safety, so that assessment of their structural integrity is very important critical for both economic and safety reasons. Eddy current testing (ECT) technique is widely used in in-service inspection of the SG tubes of NPP of pressurized water reactor type. Currently, this task is conducted by certified inspectors who interpret the ECT signals while EC probes are scanning inside the SG tubes. The interpretation of ECT signals, however, is truly a difficult task even for well-trained inspectors and accuracy of signal interpretation largely depends on their experiences and knowledge. Thus, the automated tools for the interpretation of ECT signals are strongly desired.

Many works had been done previously to develop neural network based inversion tools [1,2] since neural networks are ideally suited to the interpretation of ECT signals. The performance of any inversion system, in fact, strongly relies on the databases that had been used in the implementation of the specific system. Experimental databases are ideal, but would be very expensive and time-consuming. To address such a problem, we have proposed an intelligent, systematic inversion approach by the novel combination of neural networks and finite element (FE) ECT models. In the previous work [3-5], we had addressed following key issues that are critical for the successful application of neural networks: construction of abundant databases of ECT signals, selection of sensitive features and optimization of neural network parameters. The flaws modeled in the previous work were axisymmetric machined notch with symmetric and non-symmetric cross-sections. The proposed inversion tools showed outstanding performance for the estimation

of flaw parameters as well as for the determination of flaw types. However, the ECT signals under consideration in the previous work were limited to the synthetic ECT signals.

In the present work, quantitative characterization of flaws from the experimental ECT signals were carried out in order to validate the inversion tools proposed in the previous work. A database was constructed using the synthetic flaw signals generated by the 2 dimensional FE modeling. The hybrid neural networks of a PNN classifier [6] and three BPNN size estimators [7] were trained using the synthetic signals in the database. Experimental signals were obtained from the artificial flaws, and their magnitudes and phases were calibrated in order to compensate the gain and phase shift due to the ECT instrument. Quantitative characterization was carried out by feeding the experimental signals the trained neural networks, and their results were compared to the flaw parameters.

## DATABASE CONSTRUCTED BY FE ECT MODELS

The FE ECT models used in the present work can describe very carefully the geometry of 2D axisymmetric flaws with the variation in the depth, width and tip width, since they adopts flexible combination of quadrilateral and triangular elements [5]. Figure 1 shows the configuration of ECT applied to the Inconel 600 SG tube with a differential bobbin probe and the dimensions for FE modeling.

In the present work, we have constructed a database having 600 synthetic ECT flaw signals simulated from 2 types of symmetric flaws with the variation in the depth, width and tip width as shown in Figure 2. Two flaw types include “Inner” (ID) and “OD” (Outer)

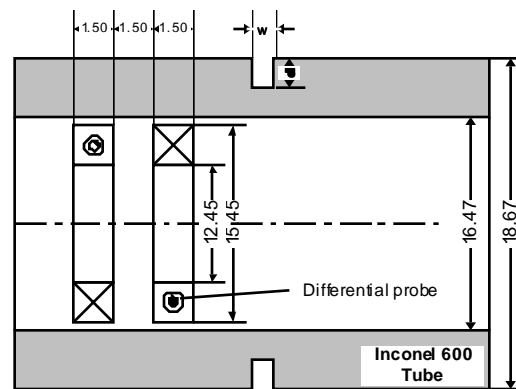


FIGURE 1. Parameters in the simulation of eddy current testing.

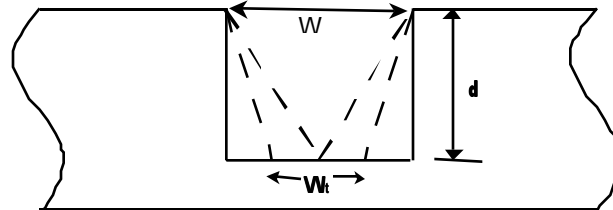


FIGURE 2. Schematic representation of cross-sections of flaws in the database.

flaws. In addition, by changing the depth, width and tip width of these flaws as listed in Table 1, a total of 300 flaws were generated, and then flaw signals were obtained with two different testing frequencies of 100 and 400 kHz.

## EXPERIMENTAL ECT SIGNALS

## Acquisition of the Experimental ECT Signals

Artificial, machined notches were fabricated in order to obtain experimental ECT signals from the flaws with well defined dimensions. Two flaw types include ID and OD flaws and by changing the depth, width and tip width as listed in Table 2, a total of 18 flaws were made. The actual dimensions of OD machined notches were measured using a measuring projector as shown Figure 3. The I- and V-shapes in Figure 3(b) and (c), respectively, were not in exact shapes of the designed flaws, and the average error of measured dimensions was 4.8 %.

**TABLE 1.** Database of the synthetic ECT flaw signals for training.

Flaw type	The Number of levels				The number of signals
	d	W	W <sub>t</sub>	f	
ID	5	5	6	2	300
OD	5	5	6	2	300
Total	-	-	-	-	600

\* d : depth (0.2, 0.4, 0.6, 0.8 and 1.0 mm)  
 \* W: width (0.2, 0.4, 0.6, 0.8 and 1.0 mm)  
 \* W<sub>t</sub>: tip width (0, 20, 40, 60, 80, 100 % of width)  
 \* f : frequency (100 and 400kHz)

**TABLE 2.** Dimensions of the machined notches, unit: mm.

Flaw type	Flaw shape	Depth	width	Tip width
ID	I	0.4	0.4, 0.6*, 0.8, 1.0	= width
	I	0.4*, 0.6, 0.8	0.6	= width
	V	0.4	1.0, 0.6	0
	V	0.6	0.4	0
OD	As same as above			

\* same flaw

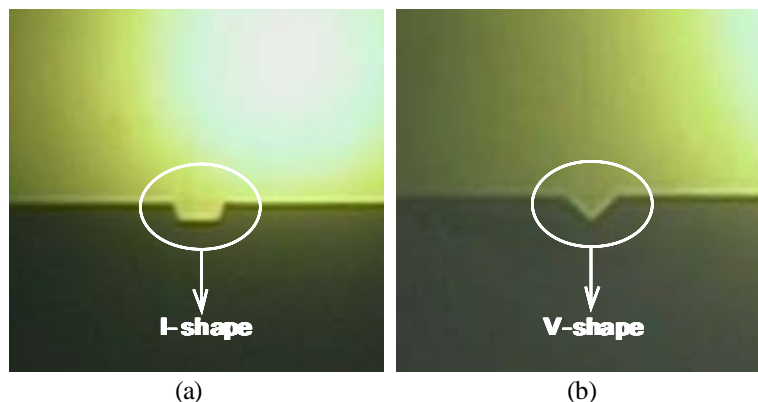


**FIGURE 3.** Measurement of the artificial flaw dimensions. (a) I-shape flaw, and (b) V-shape flaw.

## Comparison of Experimental ECT Signals to Synthetic Signals

Experimental ECT signals from the 18 machined notches were captured using a Zetec MIZ-27 ECT instrument. A total of 36 signals were obtained with two different testing frequencies of 100 and 400 kHz, and compared with the synthetic ECT signals obtained by FE modeling with the same dimensions as those of artificial flaws. Figure 4 shows typical comparisons between the experimental and synthetic signals from the I-shaped ID flaws for the test frequencies of 100 and 400 kHz. The depth of flaws was changed as 0.4, 0.6, and 0.8 mm, whereas the width of flaws was fixed as 0.6 mm. The experimental and synthetic signals show similar shape except magnitude scaling and phase rotation, which depend on the ECT instruments and should be calibrated.

### Calibration of Experimental ECT Signals

The magnitudes and phases of experimental signals should be calibrated in order to apply experimental signals to the inversion tools which have been developed using the synthetic signals. An I-shaped ID flaw with the depth of 0.4mm and the width of 1.0mm was chosen as a reference flaw. The calibration factors for the magnitude scale and phase

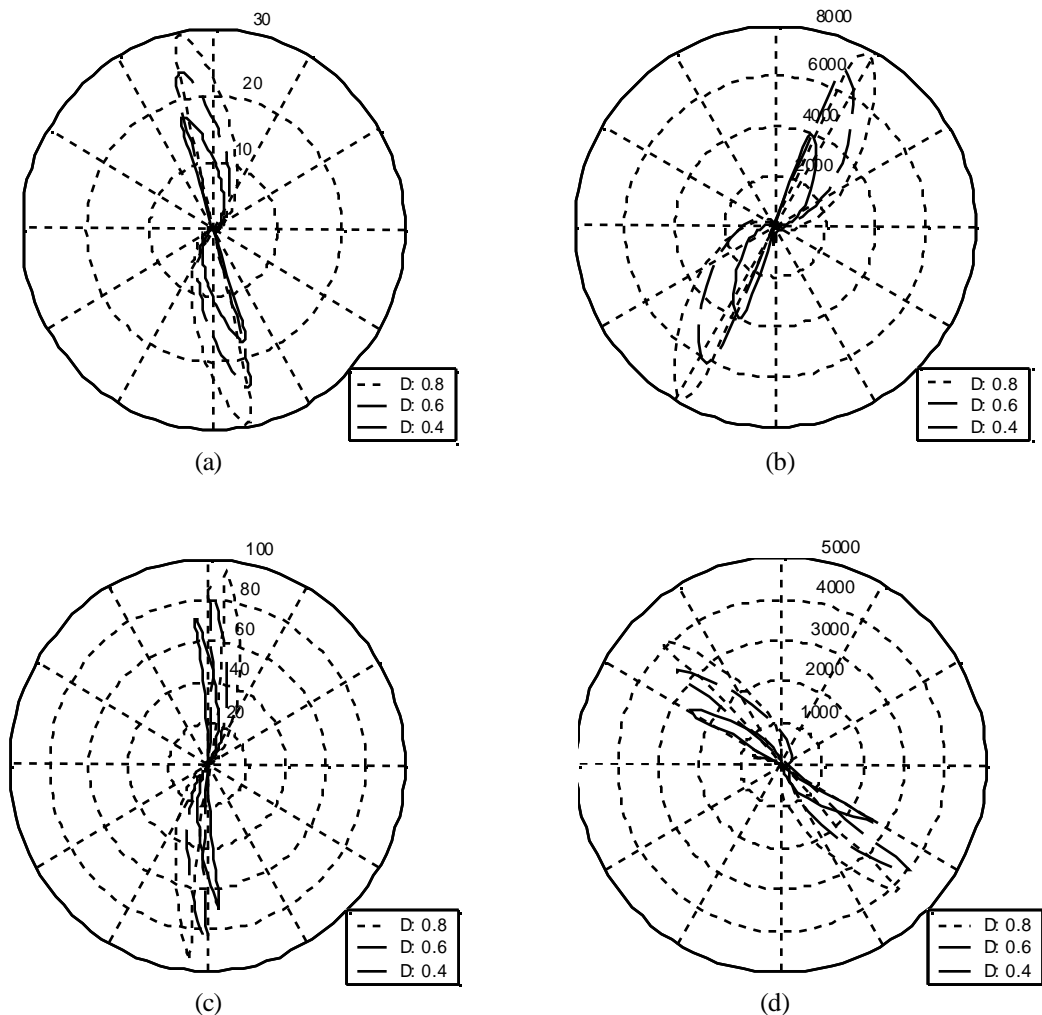


**FIGURE 4.** Comparison between synthetic and experimental signals from the ID type, I-shape flaws. (w: 0.6mm fixed, d: 0.4, 0.6, 0.8 mm). (a) and (c), synthetic signal; (b) and (d), experimental signal; (a) and (b), 100kHz test frequency; (c) and (d), 400kHz test frequency.

rotation were obtained by comparing the experimental signal from the reference flaw with the synthetic one. The calibration factors were separately obtained for each testing frequency, and applied to other experimental signals. Figure 5 shows both of the synthetic and experimental reference signals after calibration.

The magnitudes and phases of the experimental signals after calibration were compared with those of the synthetic signal, and the results were shown in Figure 6. There are good correlations between the experimental and synthetic signal, so that FE modeling of ECT seems to be valid for our purpose.

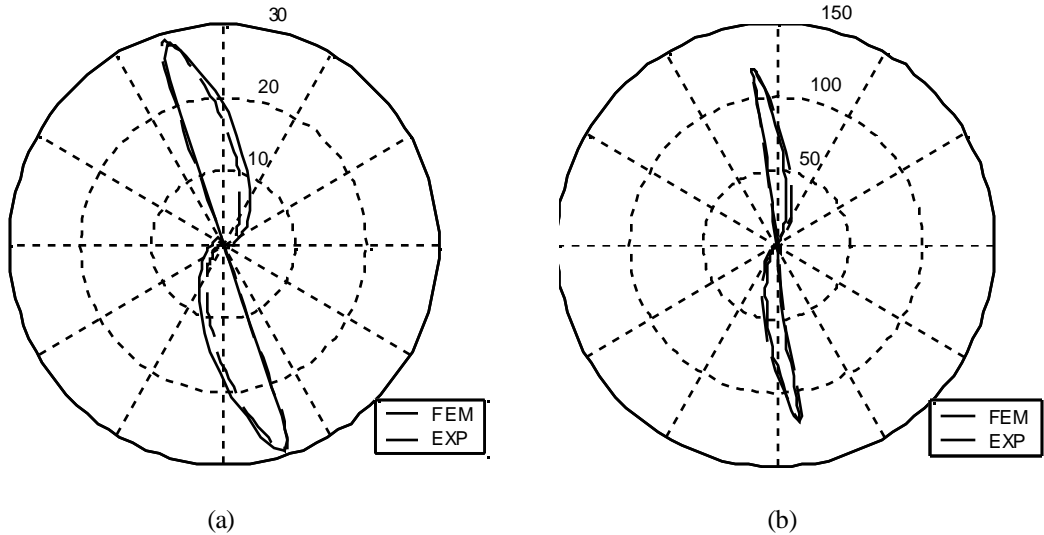


**FIGURE 5.** Comparisons between synthetic and experimental ECT signals obtained from the reference flaw after calibration. (a) 100kHz test frequency and (b) 400kHz test frequency.

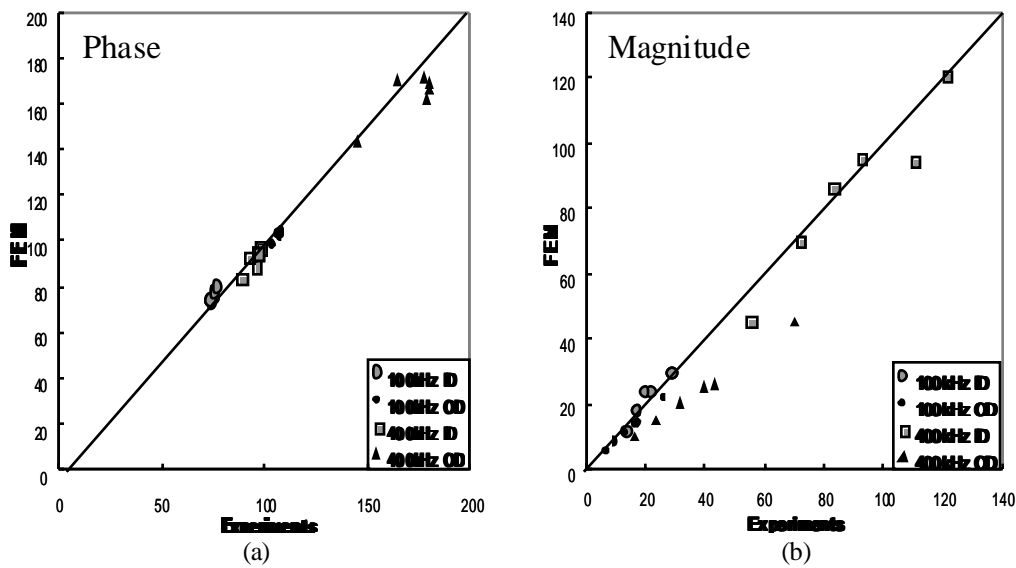


**FIGURE 6.** Correlation between synthetic and experimental ECT signals. (a) magnitude and (b) phase.

# PERFORMANCE OF CLASSIFICATION AND SIZING

## Feature Extraction and Selection

Even though it is widely recognized that features play one of the most important roles in the interpretation of ECT signals, the extraction of really “good” features, however, is not an easy task. In the present work, the features listed in the Table 3 were employed since they were verified in the previous work. A total of 11 features was defined and details of the feature selection is described in reference [3].

## Classification and Sizing

The interpretation of flaws was carried out using synthetic flaw signals in the database, with performing the flaw classification by the bPNN classifier and the flaw sizing by the BPNNs. Feature selection for classification was carried out to choose only one kind of a feature (F7), while 7 kinds of features (F1, F2, F3, F4, F5, F6 and F9) were selected for sizing of the flaw dimensions.

The PNN classifier and the three BPNN size estimators were trained based on the same training set of synthetic ECT signals, and test samples of experimental ECT signals were fed into the neural networks for the performance demonstration. The PNN showed a correct classification rate of 100%, since the discrimination between the OD and the ID flaws is relatively easy. Figure 7 summarizes the BPNN performances for the estimation of the flaw depth, width and tip width. BPNN showed excellent performance for estimating the flaw depth and width, with average errors of 0.1 mm, however, relatively lower performance for estimating the flaw tip-width, with an average error of 0.3 mm.

The actual size parameters of the fabricated flaws are, quite after, different from the design values. In that case, the performance of the BPNN will be degraded. In order to evaluate the performance of BPNN accurately, the estimated flaw parameters were compared with the measured ones. Since only the OD flaws were able to be measured their actual dimensions, the parameters of OD flaws were compared and the results are shown in Figure 8. The performances of BPNN were improved, and average errors were decreased. As results, the performances of PNN and BPNNs were satisfactory so that it can be concluded that the neural networks with database using synthetic ECT signals will be applicable to the interpretation of the experimental ECT signals.

**TABLE 3.** Features extracted from an ECT signal.

F1. Max Resistance	F2. Max Resistance angle	F3. Max Reactance
F4. Max Reactance angle	F5. Max Impedance	F6. Max Impedance angle
F7. Starting angle	F8. Ending angle	
F9. Turning phase angle at the point of maximum impedance of the signal		
F10. The length up to the maximum reactance point of the signal / The length from the maximum reactance point of the signal		
F11. Total length of the signal / Magnitude of the impedance at the maximum reactance point		

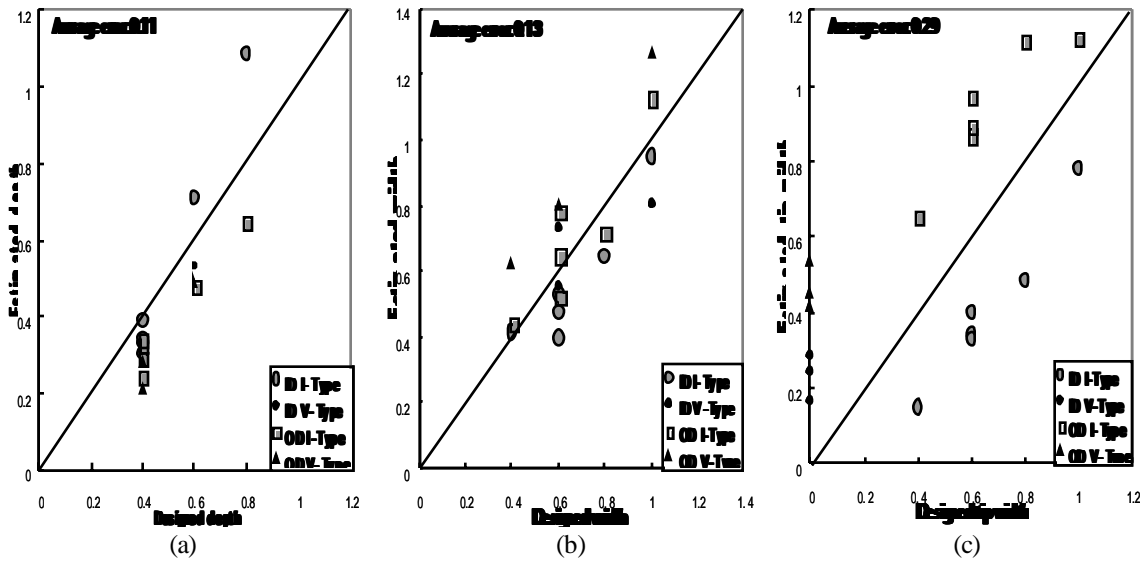


FIGURE 7. The correlations between designed and estimated flaw parameters. (a) depth, (b) width and (c) tip width.

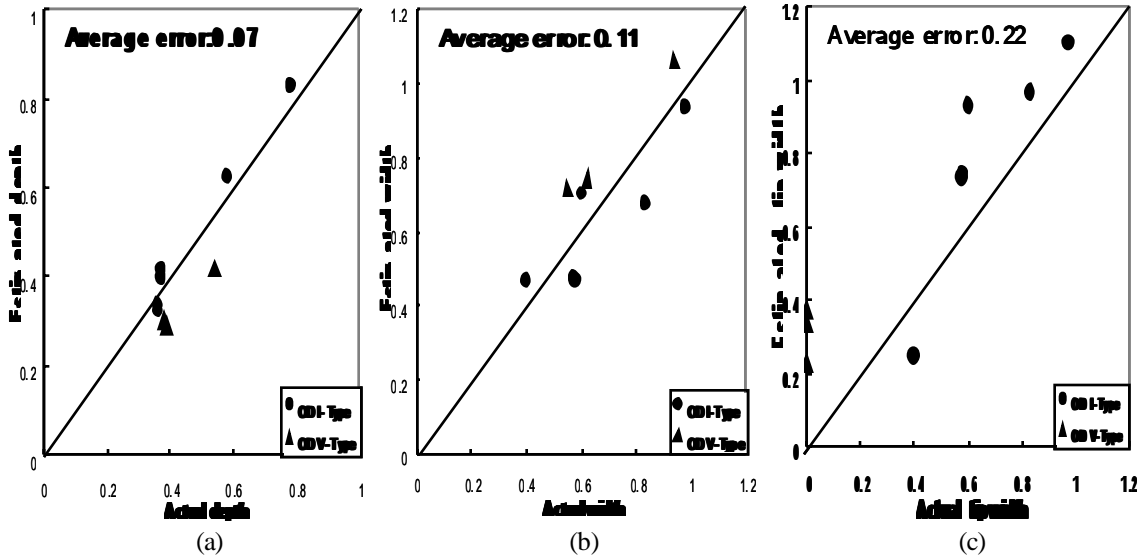


FIGURE 8. The correlations between actual and estimated flaw parameters. (a) depth, (b) width and (c) tip width.

## CONCLUSIONS

In the present work, interpretation of the experimental ECT signals was carried out in order to validate the developed, model-based inversion tools using neural networks and FE modeling of ECT. The database was constructed using synthetic flaw signals simulated by FE modeling of bobbin coil signals for axisymmetric flaws in the SG tubes. The hybrid neural networks of the PNN classifier and the three BPNN size estimators were trained using synthetic signals of the database.

Experimental signals were obtained from the 18 artificial flaws with two different testing frequencies, and calibrated to compensate the magnification and phase rotation of the ECT instrument. The interpretations of artificial flaws were carried out by feeding experimental signals into the neural networks. As results, the performances of the PNN and

BPNNs, classification of flaws and sizing of the dimensions, respectively, were excellent, so that the neural networks with database using synthetic ECT signals can be applicable to interpretation of experimental signals.

## ACKNOWLEDGMENT

The authors are grateful for the support in part provided by a grant from the Korea Science and Engineering Foundation (KOSEF), Korea Institute of Science and Technology Evaluation and Planning (KISTEP), and Safety and Structural Integrity Research Center at the Sungkyunkwan University.

## REFERENCES

1. Udpa, L. and Udpa, S. S., *Mater. Eval.* **48**, 342, 1990.
2. Shyamsunder, M. T., Rajagopalan, C., Raj, B., Dewan gan, S. K., Rao, B. P. C. and Ray, K. K., *Mater. Eval.* **58**, 93, 2000.
3. Song, S. J., Park, H. J., Shin, Y. K. and Lee, H. B., in *Review of Progress in QNDE*, Vol. 18, eds. D. O. Thompson and D. E. Chimenti, Kluwer Academic/ Plenum, New York, 1999, p.881..
4. Song, S. J., Kim, C. H., Shin, Y. K., Lee, H. B., Park, Y. W. and Yim., C. J., in *Review of Progress in QNDE*, Vol. 20, eds. D. O. Thompson and D. E. Chimenti, AIP, New York, 2001, p. 664.
5. Song, S. J. and Shin, Y. K., *NDT&E Int.* **33**, 233 2000.
6. Specht, D.F., in *Proc. of IEEE Int. Conf. on Neural Networks*, Vol. 1 1988, pp. 525-532.
7. Rumelhart, D.E., Hinton G.E. and Williams R. J., in *Parallel Distribute Processing*, ed. Rumelhart, D. E. and McClelland J. L., MIT Press, MA, 1986, pp. 318-363.